JOURNAL OF GEOPHYSICAL RESEARCH, VOL. 89, NO. B5, PAGES 3193–3200, MAY 10, 1984

Permeability of Fault Gouge Under Confining Pressure and Shear Stress

C. A. MORROW

U.S. Geological Survey

L. Q. SHI

State Seismological Bureau, People's Republic of China

J. D. BYERLEE

U.S. Geological Survey

The permeability of both clay-rich and non-clay gouges, as well as several pure clays, was studied as a function of confining pressures from 5 to 200 MPa and shear strain to 10. Permeability ranged over four orders of magnitude, from around 10^{-22} to 10^{-18} m^2 (1 darcy = 0.987×10^{-12} m^2). The lowest values were characteristic of the montmorillonite-rich and finer grained non-clay gouges. Illite, kaolinite, and chlorite had intermediate permeabilities, while the highest values were typical of the serpentine and coarser grained non-clay gouges. Grain size was an important factor in determining permeability, particularly for the clay-rich samples. The coarse grained gouges were the most permeable and decreased in permeability after shearing. Conversely, the fine grained gouges had characteristically lower permeabilities that did not vary significantly after various amounts of shearing. The permeabilities of the non-clay samples were not significantly different than those of the clays. Therefore, comminuted rock flours can be equally as effective in reducing the flow of water as the characteristically low permeability clay gouges. The strengths of the samples were quite variable. The non-clay gouges were consistently the strongest, with yield points (beginning of nonelastic behavior) around 850 MPa, while montmorillonite had an anomalously low strength in relation to all the other gouges at 250 MPa. Strength of the saturated samples under drained (low pore pressure) conditions did not correlate with high or low permeability. However, the low permeabilities of these gouges could be a factor in the measured low shear stresses along fault regions if excess pore pressures were created as a result of shearing or compaction, and this pressure was unable to dissipate through a thick section of the material.

INTRODUCTION

The fluid flow and mechanical properties of gouge materials, both clay-rich and non-clay, are of particular interest to the discussion of fault zone behavior. Clay-rich fault gouges are common and have been observed to depths of 2 km in deep mines and tunnels [*Brekke and Howard, 1973*]. Although the extent to which clays persist at greater depths is difficult to verify, *Wu et al.* [1975] and *Wang et al.* [1978] argue that clay gouges may exist to depths of 10 or 12 km and therefore greatly influence the mechanical behavior of fault zones.

Laboratory measurements [*Wang et al.*, 1980; *Summers and Byerlee*, 1977; *Morrow et al.*, 1981; *Byerlee*, 1978] have determined that clay gouges typically support lower shear stresses than most granitic rocks during frictional sliding experiments, particularly when saturated, and have extremely low frictional resistance when pore fluid movement is restricted and fluid pressures become greater than hydrostatic.

High pore pressures at depth, regardless of rock type, can lead to seismicity in areas where rocks are near failure. This condition has been identified as the cause of numerous reservoir induced earthquakes, where diffusion of impounded water into underlying rocks has triggered fault movement [*Talwani*, 1981; *Zoback and Hickman*, 1982]. In light of the obvious hazards to dams and other engineering structures adjacent to earthquake generating reservoirs, and the potentially destructive nature of natural earthquakes, the fluid flow properties of fault gouge materials as potential barriers to the migration of pore fluids merits a more detailed examination.

Paper number 3B1693.

In a previous study [*Morrow et al.*, 1981], we found that the permeability of a montmorillonite/illite-rich San Andreas Fault gouge reached values of around 10^{-22} m^2 (about 0.1 nda; 1 darcy = 0.987×10^{-12} m^2) at stresses up to 200 MPa and that the permeability did not vary significantly with shear. We wish to determine whether this rather limited observation is true of different types of gouges from other locations and whether clay-free gouges exhibit similar properties to the clays. To this end, we have investigated the permeability and shear strength of a variety of fault gouges, including pure clays, mixed-composition clay gouges, and clay-free comminuted rock gouges, with particular interest in the effect of grain size and the comparison between the clay and non-clay samples.

GOUGE DESCRIPTIONS

The gouges used in this study were collected from several locations in California along the San Andreas and nearby faults (Figure 1). The San Andreas locations included Strain Ranch (Marin County), Cienega Valley (San Benito County), Dry Lake Valley (San Benito County), Tejon Pass (Los Angeles County) and Big Pines (Los Angeles County—not to be confused with the Big Pines fault). Locations nearby but not on the San Andreas fault included the Hayward fault at D St. in downtown Hayward and near the Golden Gate bridge in San Francisco. Sampling was from surface outcrops, with the exception of the Cienega Valley and Dry Lake Valley gouges, which were taken at depths of 402 and 218 m, respectively, from holes drilled into the San Andreas

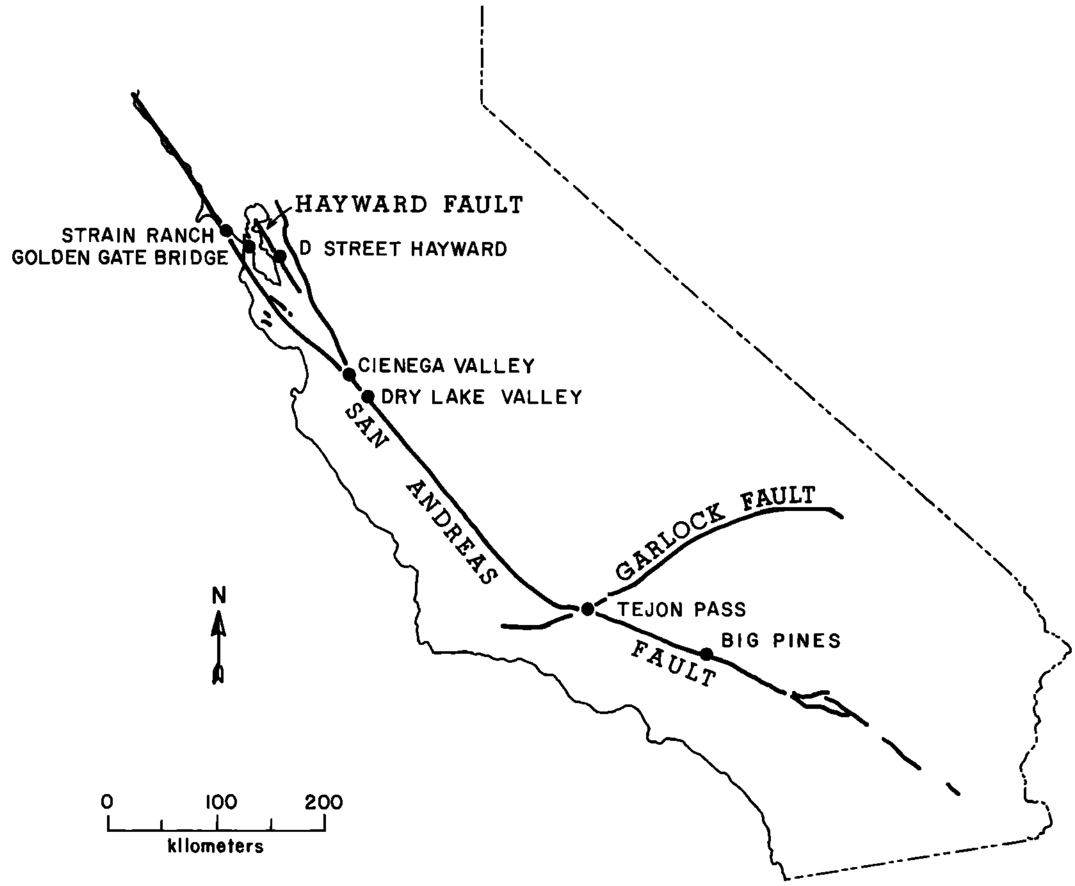

Fig. 1. Sample locations nearby and along the San Andreas fault in California.

fault [*Zoback et al.*, 1980]. Pure clays were also included in the study for comparison. These were montmorillonite (Chambers, Arizona), kaolinite (Lincoln, California), and illite (Fithian, Illinois).

Mineralogical compositions of the clay-rich gouges determined by X ray diffraction are given in Table 1. The Cienega Valley, Dry Lake Valley, and Tejon Pass samples are all similar and are composed largely of montmorillonite and mixed layer (inter-

TABLE 1. Mineralogical Composition of Gouges and Clays Mineral Percentages (wt% ± 2%)

Name of Gouge or Clay	Chlorite	Kaolinite	Illite	Montmorillonite	Mixed Layer Mont/Illite	Serpentine
Strain Ranch San Andreas Gouge Marin County	72	15	8	--	5	--
Cienega Valley San Andreas Gouge San Benito County	6	14	8	26	46	--
Dry Lake Valley San Andreas Gouge San Benito County	11	28	12	16	33	--
Tejon Pass San Andreas Gouge Los Angeles County	10	trace	20	38	32	--
D St. Hayward Fault Gouge	--	--	--	--	--	100
Golden Gate Bridge Fault Gouge	--	--	--	--	--	100
Kaolinite Lincoln, CA	--	100	--	--	--	--
Montmorillonite Chambers, AZ	--	--	--	100	--	--
Illite Fithian, IL	--	--	100	--	--	--

TABLE 2. Big Pines Gouges

Sample	Description*
BP-1	Massive gouge zone of comminuted grainite gneiss
BP-3	Black comminuted rock from a 1 cm thick shear zone in gneiss
BP-4	Pelona Schist fault slice gouge
BP-5	Granite gneiss fault slice gouge

*Whole rock analyses are given in the work of Anderson et al. [1980]

layered montmorillonite and illite) clays. The Strain Ranch gouge is chlorite-rich, and the D St. Hayward and Golden Gate Bridge samples are composed almost entirely of serpentine (chrysotile). Although there may be other types of clay-rich gouges found along the San Andreas fault, these gouges are probably representative of the wide range of mineralogies that we would expect to find.

The non-clay gouges described in Table 2 were collected from the Big Pines location, where the San Andreas fault separates granite gneiss from the Pelona Schist. These gouges are essentially a rock flour equivalent of one or the other of the parent rock compositions. Their petrogenesis is described in more detail by *Anderson et al.* [1980], who conducted the whole rock analyses of the gouges. We have maintained the same sample labeling as in their study.

Grain size analyses determined by both dry and wet sieving techniques are given in Table 3 for all the materials studied. The Cienega Valley, Dry Lake Valley, Tejon Pass, and pure clay samples were similar, being composed chiefly of clay sized particles less than 0.045 μm in diameter. The other gouge specimens had a wider distribution of grain sizes. In addition, a seived fraction of the D St. Hayward gouge was made such that all grains were less than 45 mm in diameter. In this way one can compare the effect of variable grain size between samples of like composition.

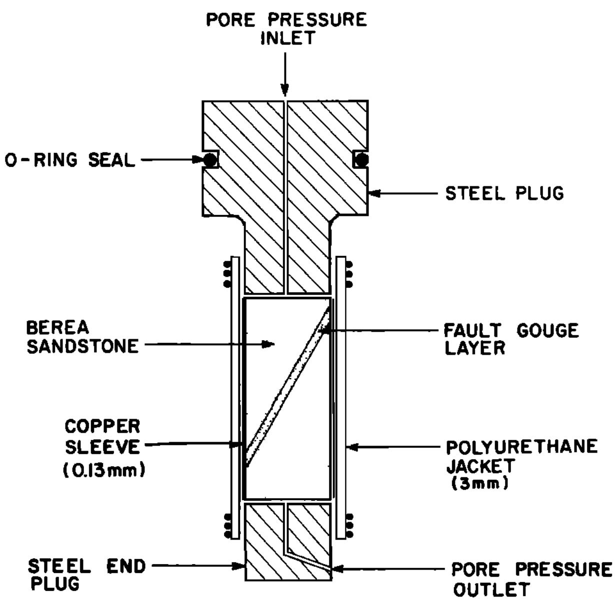

Fig. 2. Sample assembly.

EXPERIMENTAL PROCEDURE

Cylindrical samples of Berea sandstone 25.4 mm in diameter and 63.5 mm long were cut in half along a plane oriented at an angle of 30° to the axis (Figure 2). The sandstone halves were separated by a 1.0-mm thick layer of gouge along the saw cut. The gouge was presaturated with distilled water, using the same volume of water and the same procedure each time. A 0.13-mm thick copper sleeve held the two pieces of sandstone and the gouge together. The entire assembly was then jacketed in polyurethane to isolate the sample from the confining pressure fluid.

The confining pressure and inlet pore pressure were held constant by a computer controlled servo-mechanism. Pore pressure was maintained at 2 MPa at the inlet side, and atmospheric pressure at the outlet, creating a gradient across which distilled water flowed. The flow rate of water through the gouge was determined by measuring the change in volume of the pore fluid reservoir with time. Temperature was maintained at 27° ± 0.5°C throughout the system to ensure accurate pore volume measurements.

Permeability was calculated by using Darcy's law:

$$k = -\frac{q\mu}{A}\left(\frac{dP}{dx}\right)^{-1} \tag{1}$$

where q is the volumetric flow rate, μ is the dynamic viscosity of water, A is the cross sectional area normal to the direction of flow, and dP/dx is the fluid pressure gradient across the gouge. Since the permeability of Berea sandstone is many orders of magnitude higher than that of the gouge [*Zoback and Byerlee*, 1975], the pressure gradient in the sandstone was essentially zero.

Permeability was measured as a function of confining pressure for each of the specimens by increasing the hydrostatic load on the same sample in a stepwise fashion up to a pressure of 200 MPa, and then stepwise down to low pressure. After each increase or decrease in pressure, the flow rate was recorded for several hours to ensure flow equilibrium.

Using the same sample assembly as in the hydrostatic tests, permeability was determined as a function of shear displacement along the sawcut while at a confining pressure of 200 MPa. An axial load was applied to the sample at a constant axial strain rate of 10^{-6}/s over the 63.5-mm long sample, resulting in a slip rate along the gouge layer of 7.33×10^{-5} mm/s. Permeability was measured after 0.0, 0.5, 1.0, 3.0, 5.0, 7.0, and 9.0 mm of axial shortening, corresponding to a maximum shear strain in the

TABLE 3. Grain-Size Distribution of Gouges and Clays

Name of Gouge or Clay	Grain-Size Distribution (wt%)								
	2 mm	1-2 mm	0.5-1 mm	0.25-0.5 mm	0.125-0.25 mm	0.09-0.125 mm	0.063-0.09 mm	0.045-00.063 mm	0.045 mm
Strain Ranch, San Andreas	15.2	4.3	3.7	3.8	5.9	2.5	3.4	2.2	59.0
Cienega Valley, San Andreas	0.2	--	--	0.1	0.4	0.3	0.7	0.5	97.8
Dry Lake Valley, San Andreas	--	0.1	--	--	0.4	0.8	3.3	3.3	92.1
Tejon Pass, San Andreas	0.1	0.3	0.3	0.8	2.2	1.3	1.5	2.2	91.3
D St. Hayward Hayward Fault	5.1	2.1	2.6	6.3	25.2	17.5	16.8	←24.4→	
Golden Gate Bridge	0.5	1.3	3.4	13.1	37.8	18.5	←25.4→		
Kaolinite	--	--	--	--	--	--	0.2	0.2	99.6
Montmorillonite	--	--	--	--	1.0	4.4	1.9	2.8	89.9
Illite	--	--	--	--	1.3	3.0	1.4	6.1	88.2
Big Pines 1*	1	5	5	8	12	8	5	15	41
Big PInes 3*	1	4	5	10	16	8	7	14	35
Big Pines 4*	1	1	2	3	5	7	8	9	64
Big Pines 5*	2	3	4	7	10	5	5	8	56

* From Anderson et al. [1980] wt% values ± 1%

gouge layer of 10.4 at the end of the experiment. The axial load was removed for each permeability measurement. In this way, the permeability was determined as a function of shear strain without the added effect of differential stress. There was a small amount of strain recovery during unloading due to the elastic nature of the gouges, therefore measurements reflected a "maximum past strain". During these shearing experiments, the strength of the saturated gouge was also recorded. The tests were preformed under drained conditions as described in the work of *Morrow et al.* [1981]. Measurements were made after transient pore pressure changes had died away at each new confining pressure. Therefore excess pore pressure was not created in the thin gouge layer during loading that may cause a lowering of the shear strength.

RESULTS

Permeability

The permeability of the fault gouges and pure clays ranged over four orders of magnitude, as seen in Figure 3. Loading and unloading paths are indicated by the arrows on selected curves. Permeability characteristically decreased with higher confining pressure as the samples became more compacted. Upon unloading permeability values were consistently less than they were during loading.

The montmorillonite/mixed layer gouges (Tejon Pass, Dry Lake Valley, Cienega Valley, and pure montmorillonite) had the lowest permeabilities; around 10^{-21} m^2 at 200 MPa confining pressure. This set of gouges all had remarkably similar permeability values at all confining pressures regardless of the percentages of the four basic mineral constituents in each sample (Table 1). The clay-free samples BP-4 and BP-5 were also within this low permeability range. Progressively higher permeabilities were characteristic of the illite, kaolinite, and Strain Ranch samples, (5×10^{-21} to 5×10^{-19} m^2). The highest permeability gouges were the serpentine-rich Golden Gate Bridge and D St. Hayward samples and BP-1 and BP-3, with permeabilities ranging from 10^{-19} to 10^{-18} m^2, at pressures up to 200 MPa.

Permeability as a function of shear displacement is shown in Figure 4. There are three distinct types of behavior exhibited here. First, a marked reduction in permeability with displacement that is typical of the higher permeability samples (the serpentine, chlorite and kaolinite types, plus BP-1 and BP-3). These gouges all experienced an order of magnitude drop in flow rate as a result of shearing. Thin section analysis of the shear zones showed evidence of grain crushing and rotation in these coarser-grained gouges (particularly the serpentine). A second type of behavior was observed with the low permeability finer-grained montmorillonite-rich gouges (Tejon Pass, Dry Lake Valley, Cienega Valley) and to a lesser extent the pure illite sample. Here there was little change in permeability during shear. The only significant reduction in flow rate occurred during the first millimeter of sliding, as the samples compacted during the onset of shearing. Although the BP-4 and BP-5 gouges (Pelona Schist and granite gneiss) had initial permeabilities within the same range as the montmorillonite gouges, they did not exhibit a comparable behavior with strain. These two gouges, comprising the third group, showed a marked increase in flow rate after 5 mm of sliding.

Strength

From the differential stress data recorded during the displacement experiments we can plot strength curves under drained conditions at 200 MPa confining pressure (Figure 5). The strength and strain hardening characteristics of the clay samples under a

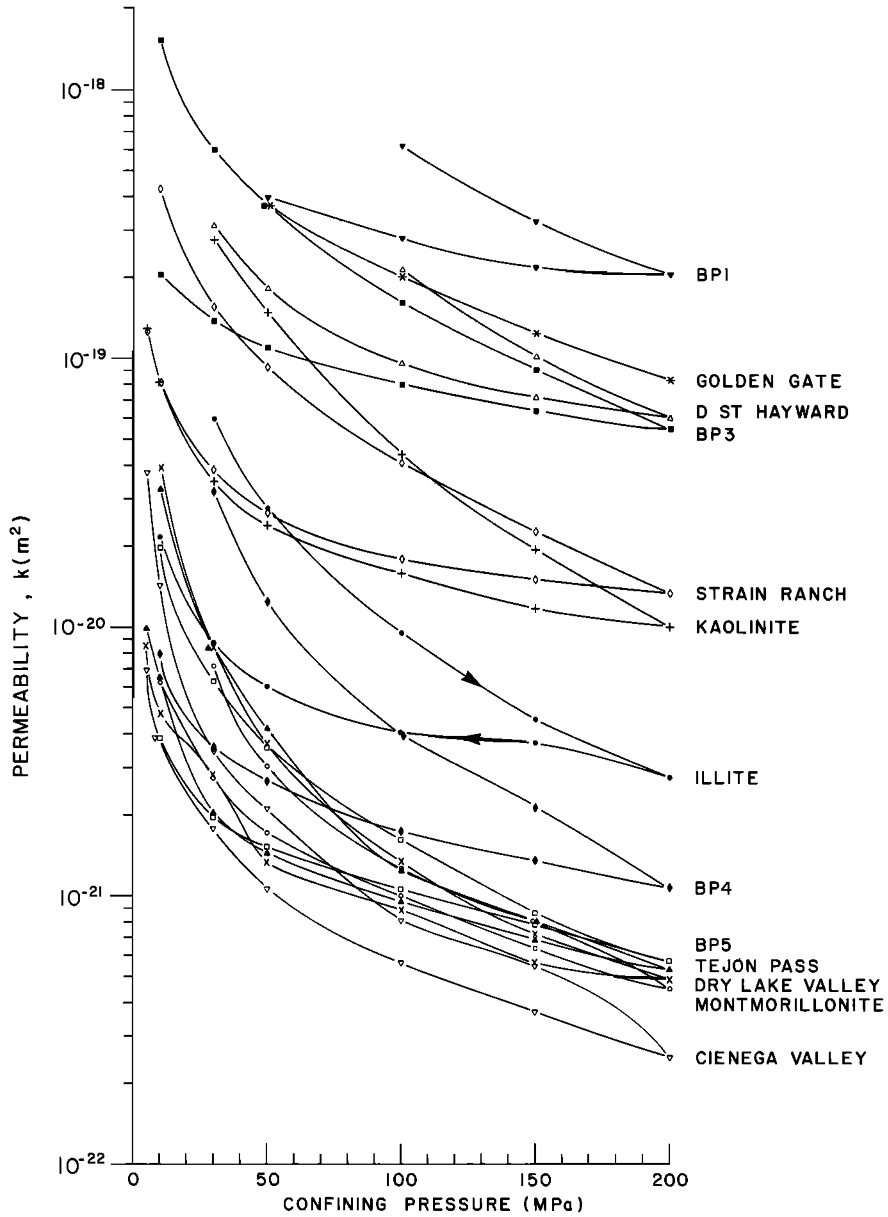

Fig. 3. Permeability of pure clays, clay-rich fault gouges, and non-clay Big Pines gouges as a function of confining pressure. The loading and unloading paths exemplary of all the samples are illustrated with arrows on the illite curve. The permeabilities of the unloading paths are consistently lower than the loading permeabilities because compaction of the grains is not completely reversible.

variety of different conditions are described in more detail in the work of *Morrow et al.* [1982]. From Figure 5, we see that the strengths of the rock-flour and clay samples were quite distinct from each other. The rock-flour samples, derived from a number of different parent materials, all have very similar stress-strain curves, and supported substantially higher frictional stresses than any of the clay samples. These values of shear strength are consistent with those previously reported for granitic type rocks [*Byerlee*, 1978].

There appears to be no systematic relation between strength and permeability for these samples. Low permeability gouges cover the entire range of frictional stress, from the lower-strength montmorillonite, to the predictably strong rock-flour gouges. Low strength can be equated with low permeability only if the samples are undrained (e.g., the gouge is thick in comparison with the time for fluid drainage or the gouge is bounded by less permeable rocks).

Discussion

The grain size distributions (Table 3) appear to be a factor in the variable permeability of all the gouges illustrated in Figure 3. The clay-rich low permeability gouges were all predominantly composed (>90%) of fine grains less than 0.045 mm in diameter. The higher permeability clay gouges, on the other hand (Golden Gate Bridge, D St. Hayward), had a more even distribution of grain sizes, from granules to clay-sized particles. Only a small percent of these grains were less than 0.045 mm in diameter. The difference in the range of grain size is not as striking with the Big Pines gouges as compared with the clays. But here again, the

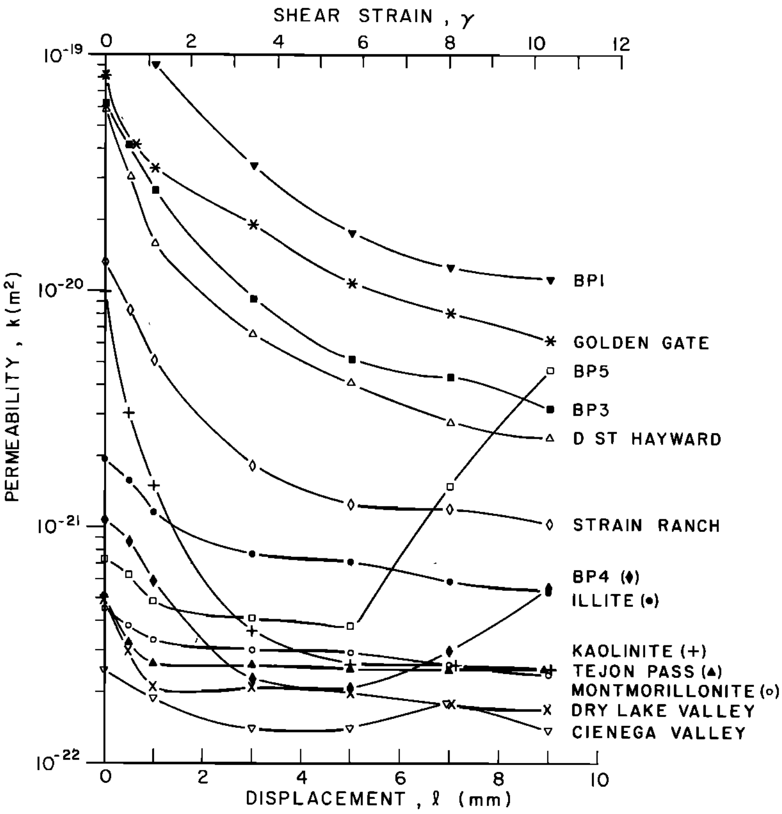

Fig. 4. Permeabilities of pure clays, clay gouges, and non- clay gouges as a function of shear strain (upper axis) and displacement (lower axis). The confining pressure during all experiments was 200 MPa. There are three types of behavior exhibited here: permeability decreases after sliding for the coarse-grained higher-permeability gouges, permeability does not change significantly for the fine-grained lower-permeability gouges, and two of the nonclay gouges show dilatant behavior after 4 mm of sliding.

more coarse samples BP-1 and BP-3 (41% and 35% grains <0.045 mm, respectively) had higher permeabilities than BP-4 and BP-5 (64% and 56% grains <0.045 mm, respectively).

This grain size-permeability relationship has been demonstrated in the past [*Beard and Weyll*, 1973; *Lambe*, 1954], for both sands and clays. We also observed this effect with the sieved fraction (all grains <45 μm) of the D St. Hayward gouge, where permeability as a function of confining pressure paralleled the unsieved gouge curves but was 63% lower. These experimental results are all consistent with the Kozeny-Carmen equation [*Bear*, 1972] which states that permeability is proportional to porosity and inversely proportional to specific surface area. *Bear* [1972] derives a number of modifications to the Kozeny-Carmen equation showing that permeability is also proportional to grain size, pore size, and crack width. Unfortunately, we have not measured all the parameters necessary to test these relationships.

We noted in the last section that the flow behavior during shearing (Figure 4) seemed to fall into groups depending on permeability range and grain size. The coarse-grained gouges decreased in permeability with shear, while the fine grained gouges did not. One interpretation of this finding may be that the coarse gouges are approaching the permeability of the finer ones as they are crushed into smaller particles and become more densly packed. Grain crushing was noted in thin section analyses of the coarser samples, particularly the serpentines. This does not explain the rise in permeability with shear in samples BP-4 and BP-5. These runs were repeated to verify their differing behavior. The increases in permeability after 4 mm of sliding could be a result of dilatancy in the samples, although we did not measure volumetric strain in order to substantiate this hypothesis. We can imagine that the rounder-shaped rock flour grains are more likely to cause dilation than the flat clay platelets as they slide past one another to accommodate shear. It must be noted that these experiments have been run on samples that have been disaggregated and then "reassembled" for studies in the laboratory. Therefore, the lower permeabilities observed after shearing due to grain alignment may be more representative of in situ permeabilities than those values obtained after hydrostatic tests.

The presence of montmorillonite may also be a factor in determining permeability. All of the clay gouges with permeabilities of 10^{-21} m^2 or less have some major percentage of this highly expandable clay. The degree to which montmorillonite swells when in contact with fluids (thereby reducing flow through the sample), is in part dependent on fluid chemistry. Previous studies [*Moore et al.*, 1982] on pure montmorillonites have shown that strong electrolyte solutions suppress the water bonding properties of clay platelets, and as a result, permeabilities can be varied by orders of magnitude in different electrolyte solutions. Since our studies on clay gouges were conducted with distilled water as the fluid medium, we feel that these results represent a lower bound on the permeabilities expected from gouges containing expandable clays.

With information on the strength and fluid flow properties of fault gouges, we should be able to address the question of what role gouges play in areas of induced seismicity. *Talwani* [1981] found that at several sites of induced seismicity in North

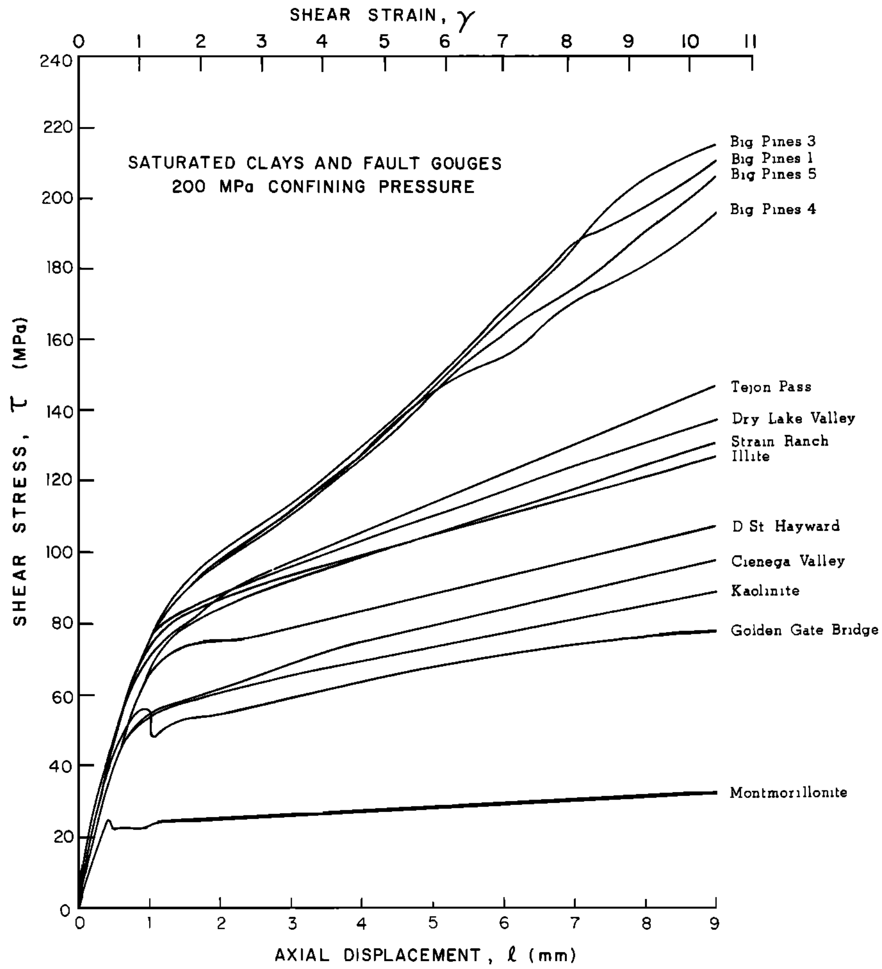

Fig. 5. Frictional strength of all samples up to 9 mm of axial shortening, or a shear strain of approximately 10.4 in the gouge layer.

Carolina, the growth of the epicentral area was linear with time, suggesting that a diffusional flow process was operating. This state can be described by the equation

$$t \simeq \frac{\ell^2}{C} \tag{2}$$

where t is the time between reservoir impoundment and seismicity, ℓ is the distance from the reservoir to the hypocenter of the earthquake, and C is hydraulic diffusivity. C is related to other physical properites by

$$C = \frac{k}{\phi\eta\beta} \tag{3}$$

where k is bulk permeability, ϕ is the average porosity of the rock, and η and β are the viscosity and compressibility of the pore fluids, respectively. The growth of the epicentral region with time in these cases would suggest that the earthquakes were caused by a pore pressure front that migrated away from the reservoir and not by the load of the reservoir on the rocks [*Talwani,* 1981]. In areas where rocks are stressed to near failure levels, this increase in pore pressure can trigger earthquakes.

Where only time and location data for a single reservoir induced earthquake event are available, the hydraulic diffusivity can be estimated by using (2) above. *Talwani* [1981] found that for over 40 cases of earthquakes caused by reservoirs and fluid injection, the hydaulic diffusivity was within an order of magnitude of 5×10^4 cm^2/s. He concluded that this may be a characteristic value associated with induced seismicity. For typical values of rock porosity, fluid compressibility, and viscosity, this diffusivity corresponds to a permeability of 10^{-16} to 10^{-14} m^2.

Using a different approach to determine C, *Zoback and Hickman* [1982], in their study of the Monticello Reservoir earthquakes in North Carolina, measured the in situ permeabilities of the rocks. These values were typically around 10^{-15} m^2 (1 millidarcy), corresponding to a diffusivity of 3×10^4 cm^2/s, using (3) with porosity, fluid viscosity, and compressibility appropriate to their site. This value of diffusivity is well within the range that Talwani found as characteristic of induced earthquakes. In addition, the time history of the Monticello earthquakes was consistent with the diffusion model of (2).

The permeability of 10^{-15} m^2 measured by *Zoback and Hickman* [1982] and inferred by Talwani using the diffusional fluid flow model is many orders of magnitude greater than the permeabilities measured for our fault gouges and is more typical of jointed rocks [*Brace,* 1980]. The high diffusivities would suggest that joints and fractures are the pathways through which fluids migrate away from reservoirs. In contrast, gouge-filled fault zones are more likely to restrict fluid flow, becoming barriers that may restrict the migration of pore fluids and thus inhibit the growth of epicentral zones in areas of induced seismicity.

The state and extent of gouge materials within active fault zones is also important to the discussion of stresses at depth. *Lachenbruch and Sass* [1980] argue that shear stresses must be low (around 10 MPa) along the San Andreas Fault, based on the absence of a heat flow anomaly across the fault. *O'Neil and Hanks* [1980], on the other hand, suggest that these stresses may be high but that water circulation convects the heat away from the fault, masking the high stresses and giving the appearance of a low-heat flow, low-stress environment. *Zoback et al.* [1980] measured in situ stresses to a depth of 1 km along the San Andreas in Southern California and found that stresses increased with depth to near 10 MPa in their deepest hole. Whether this trend can be extrapolated to greater depth, or whether stresses level off at this point as Lachenbruch and Sass would have, is a most important question.

The low permeability of our fault gouge samples would indicate that convection is probably an inefficient means of transport through rocks that contain numerous deep faults. These results show that even non-clay gouges are effective in reducing flow across fault zones. If fault gouges are extensive at depth (a point that is not yet resolved), then the low permeabilities would place restraints on the amount of heat transport we could expect away from faults by convection.

Laboratory studies of frictional sliding [*Summers and Byerlee*, 1977; *Wang et al.*, 1980] indicate that fault gouges can sustain much higher stresses than the heat flow constraint would suggest. However, undrained tests of shear strength point out that high pore pressures are quite effective in reducing the resistance to shear, particularly in samples that contain expandable clays such as montmorillonite [*Morrow et al.*, 1982].

In order to reconcile the opposing points of view presented above, we can envision two different scenarios. First, if stresses along the fault are low, then the gouge materials must be in an undrained state. This requires low permeability gouges (which we have found at least at shallow depths), and a wide and deep fault zone that will sustain high pore pressures over time. Second, if stresses along the fault are high, then the gouge materials must be in a drained state. In this case, pore fluids must be free to flow out of the fault zone, which places restraints on the geometry of the zone in question if permeabilities are low. Clearly, these questions cannot be resolved without further details on the geology and stress distribution of fault zones at depth.

SUMMARY OF RESULTS

Permeabilities of all the gouges under confining pressures up to 200 MPa ranged over four orders of magnitude. The lowest values of around 10^{-21} m^2 were characteristic of the montmorillonite-rich and finer-grained Big Pines gouges, and the highest values of between 10^{-19} to 10^{-18} m^2 were typical of the serpentine and coarser-grained Big Pines gouges. The permeability of the comminuted rock flours was not significantly different than that of the clay samples.

Grain size appears to be an important factor in controlling permeability, particularly for the clay-rich samples. The coarse-grained gouges were the most permeable and showed significant decreases in permeability with shearing. Rearrangement of the grain fabric through grain rotation, cracking and crushing was observed in thin sections of these coarse gouges layer after shearing. The fine-grained clay gouges, on the other hand, had characteristically lower permeabilities that did not vary with shearing. The fine-grained non-clay gouges (BP-4 and BP-5) exhibited an increase in permeability after 4 mm of sliding, possibly because these gouges dilated in order to accommodate the shearing of the more rounded grains.

The gouges and pure clays exhibited a wide variety of shear strengths. Montmorillonite was substantially weaker than the other clay gouges and pure clay samples. The clay-free rock-flour samples exhibited consistently higher frictional strengths that are typical of other fractured granitic rocks. Strength did not correlate with permeability, as these experiments were run under drained conditions and therefore excess pore pressures were probably not generated in the gouge zones.

REFERENCES

Anderson, J. L., R. H. Osborne, and D. F. Palmer, Petrogenesis of clastic rocks within the San Andreas fault zone of southern California, U.S.A., *Tectonophysics, 67*, 221, 1980.

Bear, J., *Dynamics of Fluids in Porous Media*, p.166, Elsevier, New York, 1972.

Beard, D. C., and P. K. Weyl, Influence of texture on porosity and permeability of unconsolidated sand, *Am. Assoc. Pet. Geol. Bull., 57*, 349-369, 1973.

Brace, W. F., Permeability of crystalline and argillaceous rocks, *Int. J. Rock Mech. Min. Sci. Geomech. Abstr., 17*, 241, 1980.

Brekke, T. L., and T. R. Howard, Functional classification of gouge materials from seams and faults in relation to stability problems in underground openings, Final report submitted to U.S.Bureau of Reclamation, Dept. of Civil Eng., Univ. of Calif., Berkeley, 1973.

Byerlee, J. D., Friction of rocks, *Pure Appl. Geophys., 116*, 615, 1978.

Lachenbruch, A. H., and J. H. Sass, Heat flow and energetics of the San Andreas Fault zone, *J. Geophy. Res., 85*, 6185, 1980.

Lambe, T. W., The permeability of fine grained soils, in *Proceedings of the ASTM Symposium on Permeability of Soils*, vol.56, 1954.

Moore, D. E., C. A. Morrow, and J. D. Byerlee, Use of swelling clays to reduce permeability and its potential application to nuclear waste repository sealing, *Geophy. Res. Lett., 9*, 1009, 1982.

Morrow, C. A., L. Q. Shi, and J. D. Byerlee, Permeability and strength of San Andreas fault gouge under high pressure, *Geoph. Res. Lett., 8*, 325, 1981.

Morrow, C. A., L. Q. Shi, and J. D. Byerlee, Strain hardening and strength of clay-rich fault gouges, *J. Geophy. Res., 87*, 6771, 1982.

O'Neil, J. R., and T. C. Hanks, Geochemical evidence for water-rock interaction along the San Andreas and Garlock Faults of California, *J. Geophys. Res., 85*, 6286, 1980.

Summers, R., and J. D. Byerlee, A note on the effect of fault gouge composition on the stability of frictional sliding, *Int. J. Rock Mech. Min. Sci. Geomech. Abstr., 14*, 155, 1977.

Talwani, P. D., Hydraulic diffusivity and reservoir induced seismicity, Final Technical Report, 48 pp., U.S. Geol. Surv., Reston, Va., 1981.

Wang, C, W. Lin, and F. Wu, Constitution of the San Andreas fault zone at depth, *Geophy. Res. Lett., 5*, 741, 1978.

Wang, C., N. Mao, and F. T. Wu, Mechanical properties of clays at high pressure, *J. Geophys. Res., 85*, 1462-1468, 1980.

Wu, F., L. Blatter, and H. Roberson, Clay gouges in the San Andreas fault system and their possible implications, *Pure Appl. Geophys., 113*, 87, 1975.

Zoback, M. D., and J. D. Byerlee, Permeability and effective stress, *Am. Assoc. Pet. Geol. Bull., 59*, 154-158, 1975.

Zoback, M. D., and S. Hickman, In situ study of the physical mechanisms controlling induced seismicity at Monticello Reservoir, South Carolina, *J. Geophys. Res., 87*,6959, 1982

Zoback, M. D., H.Tsukahara, and S.Hickman Stress measurements at depth in the vicinity of the San Andreas fault: Implications for the magnitude of shear stress at depth, *J. Geophys. Res., 85*,6157, 1980.

J. D. Byerlee and C. A. Morrow, U. S. Geological Survey, 345 Middlefield Road, Menlo Park, CA 94025.

L. Q. Shi, State Seismological Bureau, Beijing, People's Republic of China.

(Received April 8, 1983;
revised October 6, 1983;
accepted October 14, 1983.)